

Two-dimensional Hubbard-Holstein bipolaron

A. Macridin^{1,3}, G. A. Sawatzky^{1,2} and Mark Jarrell³

¹*University of Groningen, Nijenborgh 4, 9747 AG, Groningen, The Netherlands*

²*University of British Columbia, 6224 Agricultural Road, Vancouver, Canada*

³*University of Cincinnati, Cincinnati, Ohio, 45221, USA*

(Dated: November 5, 2018)

We present a diagrammatic Monte Carlo study of the properties of the Hubbard-Holstein bipolaron on a two-dimensional square lattice. With a small Coulomb repulsion, U , and with increasing electron-phonon interaction, and when reaching a value about two times smaller than the one corresponding to the transition of light polaron to heavy polaron, the system suffers a sharp transition from a state formed by two weakly bound light polarons to a heavy, strongly bound on-site bipolaron. Aside from this rather conventional bipolaron a new bipolaron state is found for large U at intermediate and large electron-phonon coupling, corresponding to two polarons bound on nearest-neighbor sites. We discuss both the properties of the different bipolaron states and the transition from one state to another. We present a phase diagram in parameter space defined by the electron-phonon coupling and U . Our numerical method does not use any artificial approximation and can be easily modified to other bipolaron models with longer range electron-phonon and/or electron-electron interaction.

I. INTRODUCTION

The interaction between electrons and lattice degrees of freedom plays a crucial role in the properties of many materials and results in a multitude of physical phenomena. Structural transitions like the cooperative Jahn-Teller distortion in perovskites, the Peierls dimerization in one-dimensional systems, or the pairing and the condensation of the charge carriers in superconductivity are some of the most spectacular effects which originate from electron-lattice interaction. Polaronic and bipolaronic effects are found in many materials like transition metal-oxides¹, superconducting materials² and conjugated polymers³. In the last years there has been growing experimental evidence that even in the fashionable strongly correlated materials like manganates and cuprates, aside from the unscreened Coulomb repulsion the electron-lattice interaction is extremely important^{4,5}.

The theoretical investigation of the interaction between charge carriers and lattice vibrations has a long history. The concept of a polaron, which describes an electron which carries with it a lattice deformation, was introduced first by Landau in 1933⁶. One of the most successful theories of the last century, the Bardeen, Cooper and Schrieffer (BCS) theory of superconductivity⁷ is based on the observation that phonons induce an effective attraction between electrons.

The discovery of high T_c superconductors renewed the interest in the study of the electron-phonon interaction, and the bipolaron problem in particular. In the cuprate materials the strength of the interaction between electrons and phonons is believed to be in the intermediate regime. Because of this rather strong interaction the lattice ions change their equilibrium position when they are in the vicinity of charge carriers, i.e. the charge carriers drive a phonon vacuum instability^{9,10}. The classical Migdal-Eliashberg approach to the theory of superconductivity⁸, which neglects these effects and is valid only

for small electron-phonon coupling, cannot be applied to cuprates. Therefore special theoretical attention was given to scenarios where electrons (or holes) form pairs in real space (bipolarons), which suffer Bose-Einstein condensation, leading to superconductivity⁹. In this respect Alexandrov and co-workers proposed the strong electron-phonon coupling theory as a starting point for explaining the physics of high T_c superconductors. In their theory^{9,11}, as a consequence of the strong electron-phonon interaction, the holes pair in bipolarons. For low charge carriers density, the system can be regarded as a charged $2e$ Bose gas which condense at T_c , resulting in superconductivity.

However the study of these systems is complicated by the failure of both strong and weak coupling perturbation theory, even for simple model systems, at intermediate coupling strength. Novel algorithms were developed to address the problem in this difficult region of parameter space. The bipolaron problem, which is defined by two electrons on a lattice, has been intensively studied in the last years. For the one dimensional case the problem was addressed by Bonča *et al.*¹³ with an exact diagonalization technique on a variationally determined Hilbert subspace. Other one-dimensional calculations were based on variational methods¹⁴ and density-matrix combined with Lanczos diagonalization technique¹⁵. The two-dimensional case was investigated in the adiabatic approximation¹⁶ and with variational methods¹⁷.

In this paper we address the Hubbard-Holstein (HH) bipolaron which is one of the simplest and most popular models which contains both electron-electron and the electron-phonon interaction. Its solution is important for understanding the competition between the phonon-induced electron-electron attraction and the electron-electron Coulomb repulsion³⁰. As our calculation, based on a Quantum Monte Carlo algorithm, shows, in the intermediate and strong electron-phonon coupling regions, phonons strongly renormalize the effective hopping in-

tegral of the electrons, strongly reduce the effective on-site Coulomb repulsion but do not significantly affect the nearest-neighbor exchange interaction. This gives rise to low-energy effective Hamiltonians with a large antiferromagnetic interaction relative to the effective hopping and the effective repulsion terms, which couldn't be derived starting from pure electronic models. We find that, depending on the value of the Coulomb repulsion, two electrons can form an on-site strongly bound state for small U or a weakly bound nearest-neighbor localized state for larger U . The former state appears when the effective on-site attraction due to phonons overcome the Coulomb repulsion and the later is a result of the exchange interaction which wins over the strongly renormalized electron (polaron) kinetic energy.

We developed a Diagrammatic Quantum Monte Carlo (DQMC) algorithm suitable for studying the two-dimensional HH bipolaron. To our knowledge, this is the first two-dimensional calculation which considers dynamical phonons and does not entail any artificial truncation of the Hilbert space. Our algorithm computes the imaginary time two-particle Green's function from which we extract information about the bipolaron state at long imaginary time. The DQMC algorithms were introduced by Prokof'ev *et al.*¹⁸ and used to calculate the properties of Fröhlich¹⁹ and spin²⁰ polarons. With the same technique the two-body problem was addressed by Burovski *et al.*²¹ for the exciton problem. Here we work in direct space (site) representation, the basis consisting of Wannier orbitals and phonons at each site. This is in contrast to the exciton problem where the electron-hole interaction is attractive allowing a momentum space calculation free of the sign problem. By working in real space we have managed to avoid the sign problem which would appear in the momentum representation when the Coulomb repulsion is introduced. The code can be easily adapted to include longer range electron-phonon or electron-electron interactions and to study models more suitable to the cuprates, as for example the extended HH model²². The disadvantage is that in this basis the momentum dependence of different quantities is difficult or sometimes impossible to compute. We consider a square lattice of 25×25 sites with periodic boundary conditions which is large enough for negligible finite size errors. There are no other truncations of the Hilbert space.

II. MODEL HAMILTONIAN

The Hubbard-Holstein Hamiltonian reads

$$H = -t \sum_{\langle ij \rangle, \sigma} (c_{i\sigma}^\dagger c_{j\sigma} + H.c) + U \sum_i n_{i\uparrow} n_{i\downarrow} + \omega_0 \sum_i b_i^\dagger b_i + g \sum_{i, \sigma} n_{i\sigma} (b_i^\dagger + b_i) . \quad (1)$$

Here $c_{i\sigma}^\dagger$ ($c_{i\sigma}$) is the creation (annihilation) operator of

an electron with spin σ at site i . b_i^\dagger , b_i are phonon creation and respectively annihilation operators at site i . The first term describes the nearest-neighbor hopping of the electrons, and the second the on-site Coulomb repulsion between two electrons. The lattice degrees of freedom are described by a set of independent oscillators at each site, with frequency ω_0 . The electrons couple through the density $n_{i\sigma} = c_{i\sigma}^\dagger c_{i\sigma}$ to the local lattice displacement $x_i \propto (b_i^\dagger + b_i)$ with a strength g . This Hamiltonian describes a tight-binding model together with an on-site Coulomb repulsion term and an on-site electron-phonon interaction term. The Holstein and the Hubbard models are limiting cases for $U = 0$ and $g = 0$ respectively.

In this paper we address the electron pairing as a function of both Coulomb repulsion and electron-phonon interaction by studying two electrons on a square two-dimensional lattice.

III. PERTURBATION THEORY RESULTS

The HH model cannot be solved analytically except for the two extreme cases of weak and strong electron-phonon interaction, when perturbation theory can be applied. The most interesting physical situation is in between these regimes. In order to understand what happens in the intermediate region, it is necessary to present first the weak and strong coupling cases.

A. Weak electron-phonon coupling

For $g = 0$, the ground state will be formed by two electrons with zero momentum moving freely through the lattice. The total spin is zero because the triplet state could not have the two electrons in the same $k = 0$ state.

When the electron-phonon interaction is switched on, two things happen. The electrons get lightly dressed which results in an increase of their effective mass, and the electron-phonon interaction introduces a frequency dependent effective attraction between the electrons. Up to second order in g the effective attraction is proportional to the phonon propagator

$$V_{eff}^{ph}(\omega) = g^2 \mathcal{D}(q, \omega) = -\frac{2g^2 \omega_0}{\omega_0^2 - \omega^2} . \quad (2)$$

This is a retarded interaction and attractive at small frequency (for $\omega < \omega_0$). In the adiabatic limit ($\omega_0 \rightarrow \infty$) where the ions are considered light and able to follow instantaneously the motion of the electrons, the effective interaction (Eq. 2) is instantaneous.

In our model the Coulomb repulsion competes with the phonon-induced attraction, resulting in a total effective interaction

$$V_{eff}(\omega) = U - \frac{2g^2\omega_0}{\omega_0^2 - \omega^2} . \quad (3)$$

In the adiabatic limit ($\omega_0 \rightarrow \infty$) the effective interaction (Eq. 3) is instantaneous with

$$V_{eff} = U - \frac{2g^2}{\omega_0} \quad (4)$$

and the situation can be described by a pure Hubbard model.

The ability of the interaction to bind the electrons into a pair is essential. It is well known that in a two-dimensional lattice any attractive instantaneous interaction will cause two electrons to bind in a pair. We are not aware of any analytical proof that this is true for a retarded interaction (finite phonon frequency), but a simple numerical calculation on a variational space which allows states with maximum one phonon shows that the binding persists for $\omega_0/t < 1$. However, the binding energy is always very small (smaller than $10^{-3}t$) and decreases roughly linearly with decreasing ω_0 . With increasing U , in adiabatic limit, the pairing persists as long as $U < 2g^2/\omega_0$. For finite ω_0 the binding energy decreases rapidly with increasing U . It is plausible that the critical U defining the pair formation to be still $2g^2/\omega_0$, but the binding energy becomes so small with increasing U that it is very difficult to resolve numerically. However, we do believe that such extremely weak bound pairs have no physical importance. Besides, when the electron-phonon coupling is increased the situation gets rapidly complicated and the calculations restricted on the variational space with a maximum of one phonon are inappropriate. The renormalization of the electron-phonon interaction vertex becomes important. Migdal's theorem⁸ applied in classical superconductivity theory is not valid here because of the absence of the Fermi sea³¹.

B. Strong electron-phonon coupling

In the strong coupling limit, the HH model may be addressed with a canonical transformation and by treating the hopping part of the Hamiltonian as a perturbation. The last three terms in Eq. (1) are diagonal in the rotated basis obtained by applying the unitary operator²³ e^S where

$$S = -\frac{g}{\omega_0} \sum_{i,\sigma} n_{i\sigma} (b_i^\dagger - b_i) . \quad (5)$$

Using formula

$$\tilde{A} = e^S A e^{-S} = A + [S, A] + \frac{1}{2}[S, [S, A]] + .. \quad (6)$$

the transformed operators become

$$\tilde{b}_i = b_i + \sum_{\sigma} \frac{g}{\omega_0} n_{i\sigma} \quad (7)$$

$$\tilde{c}_{i\sigma} = c_{i\sigma} e^{\frac{g}{\omega_0}(b_i^\dagger - b_i)} . \quad (8)$$

The Hamiltonian written in the new basis is

$$H = H_t + H_0 \quad (9)$$

with

$$H_0 = \omega_0 \sum_i \tilde{b}_i^\dagger \tilde{b}_i - \frac{g^2}{\omega_0} \sum_{i,\sigma} \tilde{n}_{i,\sigma} + \left(U - \frac{2g^2}{\omega_0} \right) \sum_i \tilde{n}_{i\uparrow} \tilde{n}_{i\downarrow} \quad (10)$$

$$H_t = -t \sum_{\langle ij \rangle, \sigma} (\tilde{c}_{i\sigma}^\dagger \tilde{c}_{j\sigma} X_i^\dagger X_j + H.c) \quad (11)$$

and

$$X_i = e^{-\frac{g}{\omega_0}(\tilde{b}_i^\dagger - \tilde{b}_i)} . \quad (12)$$

The physical meaning of this canonical transformation is a shift of the ions equilibrium position at the sites where the electrons are present

$$\langle \tilde{x}_i \rangle = \langle \tilde{b}_i^\dagger + \tilde{b}_i \rangle = \langle b_i^\dagger + b_i + \sum_{\sigma} \frac{2g}{\omega_0} n_{i\sigma} \rangle = \langle x_i \rangle + \frac{2g}{\omega_0} \langle n_i \rangle . \quad (13)$$

As can be seen from the second term of Eq. 10, the lattice deformation energy gained due to the electron presence is

$$E_p = g^2/\omega_0 . \quad (14)$$

The dimensionless electron-phonon coupling constant may be defined as the ratio between this energy and the bare electron kinetic energy which is proportional to the hopping t and with the lattice dimensionality z . We define it as³²

$$\alpha = \frac{g^2}{\omega_0 z t} = \frac{g^2}{2\omega_0 t} . \quad (15)$$

Since the electron hopping is accompanied by a change in ions equilibrium position (see the term $X_i^\dagger X_j$ in Eq. 11), it is exponentially reduced for large g .

$$t_{eff} = t \langle i | \tilde{c}_i^\dagger \tilde{c}_j X_i^\dagger X_j | j \rangle = t e^{-\frac{g^2}{\omega_0^2}} = t e^{-\frac{\alpha z t}{\omega_0}} \quad (16)$$

The effective on-site interaction between electrons is

$$U_{eff} = U - 2\frac{g^2}{\omega_0} \equiv U - 2E_p \quad (17)$$

(the same as in Eq. (4)), and in the adiabatic limit (when $\omega_0, g \rightarrow \infty$, $g/\omega_0 \rightarrow 0$ and $2g^2/\omega_0$ is finite) $X_i = 1$ and the model can be mapped again in a pure Hubbard one.

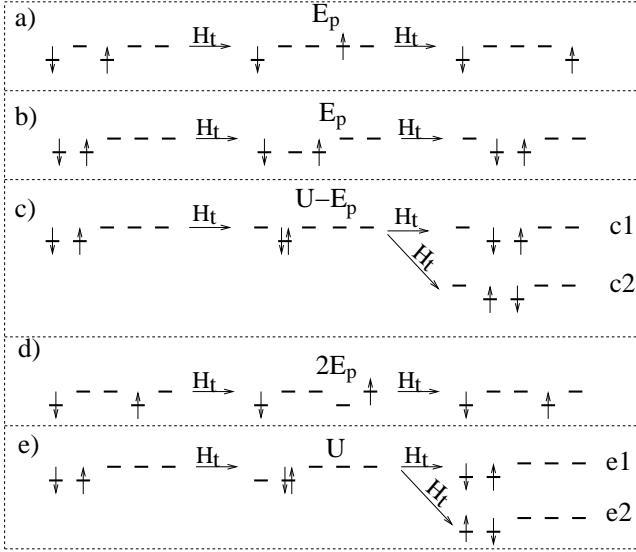


FIG. 1: Schematic representation of second order processes in H_t which determine the elements of matrix T . The small horizontal lines represent the lattice sites. If an electron is on a particular site then the equilibrium position of the ion at that site will be changed, and we indicate this by a downwards shift. The excitation energy of the intermediate state is shown above every process. If the initial and the final lattice configurations are different, the corresponding matrix element will be exponentially reduced. In the large g limit the corresponding matrix elements are: a) $-\frac{t^2}{E_p}e^{-g^2/\omega_0^2}$. b) $-\frac{t^2}{E_p}e^{-g^2/\omega_0^2}$. c) $-\frac{t^2}{U-E_p}e^{-g^2/\omega_0^2}$. d) $-\frac{t^2}{2E_p}$. e) $-\frac{t^2}{U}$.

For negative U_{eff} it is evident that the electrons form a bound state. However, based on second order perturbation theory in the hopping H_t , it can be shown that even for positive U_{eff} a stable bipolaron state can exist. Let's consider the case of large U which results in $U_{eff} > 0$. The ground state of H_0 is formed by the degenerate states

$$|a_i\rangle = c_{i\uparrow}^\dagger c_{i+a\downarrow}^\dagger |0\rangle, \quad a \neq 0. \quad (18)$$

The meaning of this notation is that the electron with spin \downarrow is at a distance “ a ” from the one with spin \uparrow residing at site “ i ”. “ a ” can take all the possible values except 0. In first order perturbation theory, the calculation of the matrix $\langle a_i | H_t | b_j \rangle$ reduces to the calculation of Eq. 16 and indicates an exponentially reduced nearest-neighbor hopping. Second order perturbation theory stabilizes the bipolaron states. It is equivalent to diagonalizing the operator

$$T = H_t \frac{1}{E_0 - H_0} H_t \quad (19)$$

on the subspace spanned by all the degenerate states of H_0 . The processes which can take place are shown schematically in Fig. 1. We can classify them in two classes. The first class includes processes as in Fig. 1-a, -b and -c, where the final lattice configuration is different

from the initial one. This results in an exponential reduction of the matrix elements, so that we can neglect them in first approximation. The second class includes processes like the ones in Fig. 1-d and -e where the initial and the final lattice configuration is unchanged. They are not exponentially reduced. In Fig. 1-d an electron hops on a neighboring site without carrying the lattice deformation around it and afterwards comes back. The energy of the intermediate state is $2E_p$, because it contains a site with deformation and without electron, and a site with an electron and without deformation. The gain in energy is $-t^2/2E_p$. This process only contributes to the diagonal elements of T . In Fig. 1-e one electron hops without carrying the lattice deformation on the neighboring site which is occupied by the other electron. The intermediate state contains a doubly occupied site which has a deformation corresponding to only one electron and a site with deformation and without electron, therefore the energy of this state is $U_{eff} + 2E_p = U$. The final state can be identical with the initial state (Fig. 1-e1), and the process contributes to the diagonal elements $T_{\delta,\delta}$, or the final state can have the electrons interchanged (e.g.: from the initial $|\uparrow, \downarrow\rangle$ to the final $|\downarrow, \uparrow\rangle$ - Fig. 1-e2), and this process contributes to the non-diagonal elements $T_{\delta,-\delta}$. δ means nearest-neighbor here. The energy gain corresponding to each of the two processes shown in Fig. 1-e is $-t^2/U$. Neglecting the exponentially reduced terms in the calculation of T , what remains is the diagonal terms and the off-diagonal ones which connect the states $|\delta\rangle$ and $|\delta\rangle$.

$$\begin{aligned} T_{a,a} &= 8 \times \left(-\frac{t^2}{2E_p}\right) & a \neq 0, 1 \\ T_{\delta,\delta} &= 6 \times \left(-\frac{t^2}{2E_p}\right) + 2 \times \left(-\frac{t^2}{U}\right) & (20) \\ T_{\delta,-\delta} &= 2 \times \left(-\frac{t^2}{U}\right) & \delta = 1 \end{aligned}$$

Solving the secular equation, we find the condition for the bipolaron existence to be

$$U < 4E_p \quad (21)$$

and the bipolaron binding energy

$$\Delta_b = -\frac{t^2}{E_p} + \frac{4t^2}{U}. \quad (22)$$

Notice that even though the bipolaron exists up to a large value of U it is a weakly bound state when $U_{eff} > 0$.

The physical interpretation of these results is simple. The energy given by Eq. 22 corresponds to a double degenerate singlet state formed by two electrons on nearest-neighbor sites. One state is a singlet along the X direction and the other along the Y direction. In distinction to Hubbard model where the exchange energy can never win over the kinetic energy and therefore cannot bind two electrons, here the interaction with phonons results in a strong reduction of the electron bandwidth but not of the exchange energy because it implies virtual transitions of electrons on double occupied sites *without carrying the*

lattice deformation with them. Therefore now the exchange energy can easily win and produce singlet bound states. However there is another effect which introduces an effective repulsion between two nearest-neighbor electrons and wins over the exchange energy when $U \geq 4E_p$. A virtual transition of an electron to an empty nearest-neighbor site without carrying the lattice deformation will lower its energy by $-t^2/2E_p$ (Fig. 1-d). But if the nearest-neighbor site is occupied by the other electron this process is not possible resulting in an effective repulsion of t^2/E_p between two nearest-neighbor electrons. Therefore Eq. 22 reflects the competition between this effective repulsion and the exchange attraction equal to $-4t^2/U$.

When the processes shown in Fig. 1 -a, -b and -c are taken into account the degeneracy of the two singlets is lifted, and two states are formed. This results in a ground state with *s*-wave (A_{1g}) symmetry and another state with *d*-wave (B_{1g}) symmetry. It should also be mentioned that if a positive next-nearest-neighbor hopping t' is introduced in the model, the *d*-wave symmetry state will be stabilized and it becomes the ground state when t' is large enough.

Let's summarize the strong coupling regime physics, neglecting at the beginning the exponentially reduced terms. When U is small the ground state energy is $U - 4E_p$ and consists of two electrons located on the same site. The first excited state contains one more phonon and has an energy $U - 4E_p + \omega_0$ (this is a N degenerate state because the phonon can be at any site). When U is increased and $U - 4E_p + \omega_0$ becomes larger than $-2E_p$ (which is the zero order energy of two electrons staying on different sites), the first excited state is a double degenerate nearest-neighbor singlet. When the hopping is switched on the low-energy physics can be described by the Hamiltonian

$$H = -t_{eff} \sum_{\langle i,j \rangle, \sigma} (c_{i\sigma}^\dagger c_{j\sigma} + H.c) + J \sum_{\langle ij \rangle} (\mathbf{S}_i \mathbf{S}_j - \frac{n_i n_j}{4}) + V \sum_{\langle i,j \rangle} n_i n_j + U_{eff} \sum_i n_{i\uparrow} n_{i\downarrow} + H' \quad (23)$$

with the hopping $t_{eff} = t e^{-g^2/\omega_0^2}$, the exchange $J = \frac{4t^2}{U}$, the nearest-neighbor repulsion $V = \frac{t^2}{E_p}$ and the on-site interaction $U_{eff} = U - 2E_p$. H' describes the processes shown in Fig. 1 -a, -b and -c. Their magnitude is either $\frac{t_{eff}}{E_p}$ or $\frac{t_{eff}}{U - E_p}$ (see the caption of Fig. 1), which is much smaller than t_{eff} . In the literature^{13,16} the bipo-

laron with the electrons located on the same site is called $S0$, and the one with the electrons located on nearest-neighbor sites $S1$. The Hamiltonian (23) describes the transition from the $S0$ to the $S1$ bipolaron in strong coupling regime. For small (i.e. negative) U_{eff} the order of the lowest energy states is: *s*-wave $S0$, *s*-wave $S1$, *d*-wave $S1$. When U_{eff} increases the $S0$ state starts mixing with *s*-wave $S1$ state. The mixing between the $S0$ and the *s*-wave $S1$ states is of order of t_{eff} , and the splitting between the *s*-wave and the *d*-wave $S1$ states is given by H' , thus being much smaller. The order of low-energy states becomes: linear combination of *s*-wave $S0$ and $S1$, *d*-wave $S1$, linear combination of *s*-wave $S0$ and $S1$. For larger U only two bound states exists: *s*-wave $S1$ and *d*-wave $S1$. In conclusion, the ground state evolves analytically (crossover) from $S0$ bipolaron to *s*-wave $S1$ bipolaron with increasing U . The situation is different for the first excited state. Here at a critical value of U , a non-analytical transition takes place, and the first excited state changes from *s*-wave symmetry to *d*-wave symmetry.

IV. ALGORITHM

A. General approach

Our algorithm calculates different imaginary time Green's functions and relies upon the ability to project out the ground state properties by extrapolating to long complex times. Let's consider the equation

$$\langle \psi | e^{-\tau H} | \psi \rangle = \sum_{\nu} |\langle \psi | \nu \rangle|^2 e^{-\tau \mathcal{E}_{\nu}} \quad (24)$$

where $|\psi\rangle$ is a whatever state and $\{|\nu\rangle\}$ form the complete set of the eigenstates with energies \mathcal{E}_{ν} . We see that at large τ Eq. 24 converges to

$$|\langle \nu_0 | \psi \rangle|^2 e^{-\tau \mathcal{E}_{\nu_0}} \quad (25)$$

where $|\nu_0\rangle$ is the ground state of the system. Suppose the ground state is separated from the first excited state by a gap Δ . We can obtain the ground state energy and the overlap of the ground state with $|\psi\rangle$ with an accuracy better than 1% (for example) calculating Eq. 24 at a time $\tau \approx 5/\Delta$.

Because the total momentum K is a quantity which is conserved in our problem we can obtain the lowest energy in the K channel by calculating

$$P^n(K, \tau) = \sum_{k, q_1, \dots, q_n} \langle (K - k - q_1 - \dots - q_n)_{\downarrow}, k_{\uparrow}; q_1, \dots, q_n | e^{-\tau H} | (K - k - q_1 - \dots - q_n)_{\downarrow}, k_{\uparrow}; q_1, \dots, q_n \rangle \rightarrow \sum_{k, q_1, \dots, q_n} |\langle (K - k - q_1 - \dots - q_n)_{\downarrow}, k_{\uparrow}; q_1, \dots, q_n | \nu_{0K} \rangle|^2 e^{-\tau E(K)}$$

at large τ . Here $|k_{1\downarrow}, k_{2\uparrow}; q_1, q_2, \dots, q_n\rangle$ is a state with two electrons, one with momentum k_1 and spin down and the other with momentum k_2 and spin up, and with n phonons with momentum q_1, q_2, \dots and q_n respectively. $|\nu_{0K}\rangle$ is the ground state (the state with the lowest energy) in the K channel. The calculation of $P^n(K, \tau)$ yields both the bipolaron energy and the n -phonon configuration probability in the bipolaron state.

For reasons related with the sign problem (to be discussed later), we calculate $P^n(K, \tau)$ in real-space representation

$$P^n(K, \tau) = \frac{1}{N} \sum_{i,x,l_1,l_2,\dots,l_n} e^{iKx} \langle i | e^{-\tau H} T_x | i \rangle \quad (27)$$

where

$$|i\rangle \equiv |i_{\downarrow}, (i+a)_{\uparrow}; i+l_1, i+l_2, \dots, i+l_n\rangle \quad (28)$$

is a state with a spin down electron at site i , a spin up electron at site $i+a$ and phonons at sites $i+l_1, i+l_2, \dots$ and $i+l_n$, and

$$T_x |i\rangle = |i+x_{\downarrow}, (i+x+a)_{\uparrow}; i+x+l_1, i+x+l_2, \dots, i+x+l_n\rangle \quad (29)$$

is the state $|i\rangle$ translated with the vector x .

Another quantity which is conserved is the total spin. Therefore for the singlet we calculate

$$P_s^n(K, \tau) = \frac{1}{N} \sum_{i,x,l_1,l_2,\dots,l_n} e^{iKx} \langle i_s | e^{-\tau H} T_x | i_s \rangle \quad (30)$$

with

$$|i_s\rangle \equiv |(i, i+a)_s; i+l_1, i+l_2, \dots, i+l_n\rangle \quad (31)$$

where $(i, i+a)_s$ is the singlet state with electrons at sites i and $i+a$. Similar equations can be written for the triplet channel.

In order to calculate the above quantities, we developed a DQMC code which stochastically generates terms of the form

$$G_{ij}(\tau) = \langle i | e^{-\tau H} | j(i, x) \rangle \quad (32)$$

where $|i\rangle$ is a general state as in Eq. 28 with two electrons at arbitrary distance from each other and with an arbitrary number of phonons. The state $|j(i, x)\rangle$ can be obtain either by applying a translation operation with an arbitrary vector x on $|i\rangle$ (i.e.

$|j\rangle = T_x |i_{\downarrow}, (i+a)_{\uparrow}; \text{phonons}\rangle$) or by applying a permutation (interchanging the electrons position) and a translation on $|i\rangle$ (i.e. $|j\rangle = T_x |i+a)_{\downarrow}, (i)_{\uparrow}; \text{phonons}\rangle$).

The value of an observable A in a particular K and S channel is

$$A(K) = \frac{1}{M} \sum_m e^{iKx(m)} g^S(m) a(m) = \frac{\sum_m e^{iKx(m)} g^S(m) w(m) a(m)}{\sum_m w(m)} \quad (33)$$

In Eq. 33 we sum over all m generated configurations with the weight $w(m)$. M is the total number of measurements, $x(m)$ is the translation vector which correspond to the configuration m , $a(m)$ is the estimator of A and $g^S(m)$ is the factor which separates the triplet from the singlet. For singlet $g^S(m)$ is 1 when electrons are on the same site and 1/2 otherwise. For triplet $g^S(m)$ is zero when the electrons are on the same site, and otherwise, 1/2 when $|j\rangle$ is a translation of $|i\rangle$ and $-1/2$ when $|j\rangle$ is a translation of a state obtained from $|i\rangle$ by interchanging the electrons position.

B. Implementation

Let's start from the Hamiltonian (1), and consider

$$H_0 = \omega_0 \sum_i b_i^\dagger b_i + U \sum_i n_{i\uparrow} n_{i\downarrow} \quad (34)$$

as the noninteracting part of the Hamiltonian. H_0 is diagonal in the real space representation. The evolution operator can be written as

$$e^{-\tau H} = e^{-\tau H_0} S(\tau) \quad (35)$$

with

$$S(\tau) = \sum_{n=0}^{\infty} \frac{(-1)^n}{n!} \int_0^\tau \dots \int_0^\tau d\tau_1 \dots d\tau_n T[H_1(\tau_1) \dots H_1(\tau_n)] \quad (36)$$

where $H_1 = H - H_0$ in the interaction picture is

$$H_1(\tau) = e^{\tau H_0} H_1 e^{-\tau H_0} \quad (37)$$

Eq. 32 becomes:

$$G_{ij}(\tau) = \langle i | e^{-\tau H} | j \rangle = e^{-\varepsilon_i \tau} \sum_{n=0}^{\infty} \frac{(-1)^n}{n!} \int_0^{\tau} \int_0^{\tau} \dots \int_0^{\tau} d\tau_1 \dots d\tau_n T[\langle i | H_1(\tau_1) H_1(\tau_2) \dots H_1(\tau_n) | j \rangle] \quad (38)$$

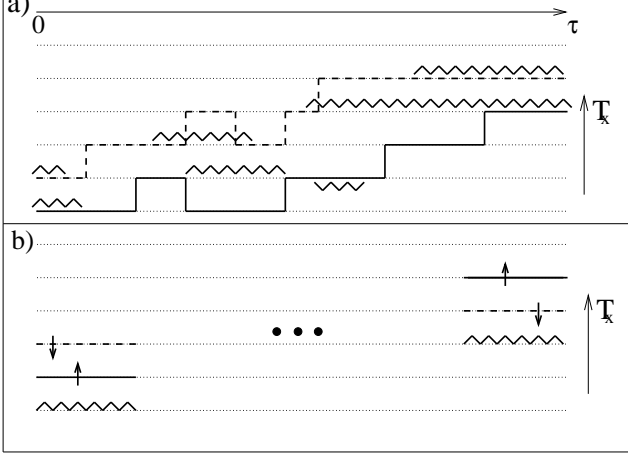


FIG. 2: a) A typical diagram which represents a term in Eq. (38). The solid line (dashed line) represents a spin up (down) electron. The wavy line is a phonon propagator. The end at time τ is a translation with the vector x of the end at time 0. b) The final state is a translation of the state obtained from initial state with the electrons position interchanged. In the code we consider only configurations where the final state is a translation of the initial state as in a) or is a translation of the state obtained from initial state with the electrons position interchanged as in b).

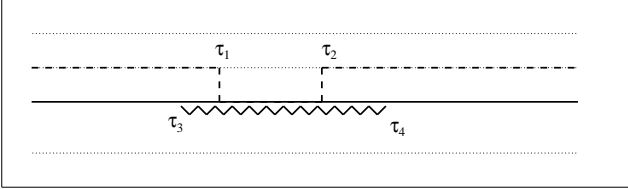


FIG. 3: The weight of this diagram is $(td\tau)^2 e^{-U(\tau_2 - \tau_1)} (gd\tau)^2 e^{-\omega(\tau_4 - \tau_3)}$. The weight of a diagram is determined by the following rules: (i) every electron hopping corresponds to a term $t d\tau$, (ii) every electron-phonon vertex corresponds to a term $g d\tau$, (iii) every phonon propagator of length $\Delta\tau$ corresponds to a term $e^{-\omega_0 \Delta\tau}$, and (iv) every interval where the electrons are on the same site during a time $\Delta\tau$ corresponds to a term $e^{-U \Delta\tau}$.

The calculation of $G_{ij}(\tau)$ is reduced to a series of integrals, with an ever increasing number of integration variables. It is easy to show that every term in Eq. (38) can be represented by a diagram and a set of simple rules can be derived to determine the diagrams weight. Typical examples of such diagrams are presented in Fig. 2. Aside from a translation, the electronic configuration at

the diagram ends must be either identical (Fig. 2-a) or with the electrons position interchanged (Fig. 2-b). The rules for determining the diagram weight are given in the caption of Fig. 3.

We generate all the possible diagrams with an arbitrary number of phonons, and with the difference between 0 and a τ_{max} chosen large enough to project the ground state. Our code is a continuous time code (i.e. it does not require artificial discretization of the imaginary time axis), and the diagrams are generated in a manner similar to that described in^{18,19,21}.

Estimators for energy, effective mass, phonon distribution and correlation function of the electrons position can be easily found. The measurements are taken only at large time where the ground state is projected out. The bipolaron energy estimator is¹⁸

$$E(m) = \frac{1}{\tau_m} (\omega_0 \sum_{i_{ph}} \tau_{i_{ph}} + U \sum_{j_U} \tau_{j_U} - N_{vertex} - N_{hop}) \quad (39)$$

where τ_m is the time (length) of the m diagram, i_{ph} counts the phonons propagators with $\tau_{i_{ph}}$ length, j_U counts the intervals with double occupied sites with τ_{j_U} length, N_{vertex} is the number of electron-phonon vertices and N_{hop} is the number of electron hopping jumps. The estimator for the inverse of the bipolaron effective mass is

$$\frac{2m_e}{m^*}(m) = \frac{x(m)^2}{\tau_m} \quad (40)$$

where $x(m)$ is the translation vector between the time 0 end and the time τ_m end. m_e is the free electron effective mass. The probability to have n phonons is calculated with the estimator

$$z^n(m) = \delta_{n_m, n} \quad (41)$$

where n_m is the number of phonons at the ends of the diagram. The electrons relative positions correlation function defined as

$$C(r) = \frac{1}{N} \sum_i \langle n_i n_{i+r} \rangle \quad (42)$$

has the estimator

$$C(r; m) = \delta_{r, R_m} \quad (43)$$

where R_m is the relative distance between electrons at the ends of the measured diagram.

As an illustration of our method, in Fig. 4 we show $\ln(P_s(0, \tau) * e^{\mu\tau})$ versus τ where

$$P_s(0, \tau) * e^{\mu\tau} = \sum_n P_s^n(0, \tau) * e^{\mu\tau} = \sum_\nu e^{-(E_\nu - \mu)\tau} \quad (44)$$

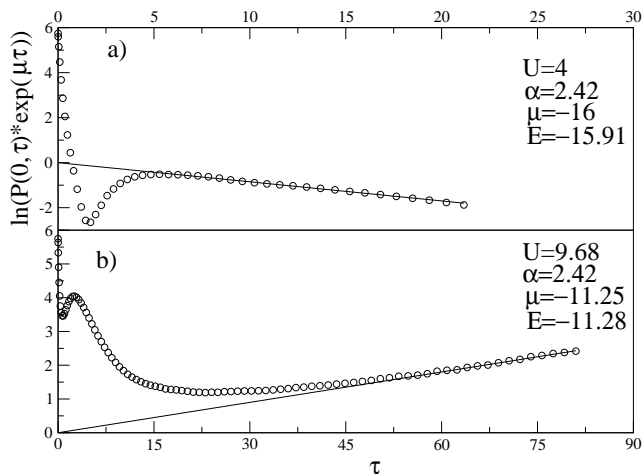


FIG. 4: $\ln(P_s(0, \tau) * e^{\mu\tau})$ versus τ . a) For the given parameters a large bipolaron binding energy results. b) For the given parameters a small bipolaron binding energy results. The linear asymptotic behavior starts at smaller time in case a). Notice that the time scale is different for the two cases presented.

with P_s^n defined in Eq. (30) for the $K = 0$ channel. μ is an arbitrary parameter which is chosen close to the bipolaron energy to avoid the exponentially small weight of the large time diagrams. It can be seen that at long imaginary time $\ln(P_s(0, \tau))$ becomes linear in τ , the slope being proportional to the ground state energy. An important remark should be made about the strong drop seen in $P_s(0, \tau)$ at short time. This is due to the fact that we generate only connected diagrams (diagrams where the phonon propagators are always glued to the electron propagator). The disconnected diagrams have an exponentially small contribution at large time, therefore they can be safely neglected, but at small time their omission will result in a strong potential drop which will not allow an efficient sampling for both long and short time diagrams. We have eliminated this problem using a fictitious potential renormalization¹⁸.

C. Discussions

In order to avoid the sign problem, our code calculates the Green's functions in the real-space representation (Wannier basis), even though this representation has some disadvantages. A similar expression to Eq. 38 can be written in the momentum space (Bloch basis), and similar rules for determining the diagrams weight can be found. This approach was considered in²¹ for the exciton model calculation. The problem with our model is that, unlike in the exciton case where the conduction-electron valence-hole interaction is attractive, we have a repulsive interaction. This will make all the diagrams with an odd number of electron-electron interaction vertices negative, which implies a very severe sign problem. In the real-

space representation the sign problem is avoided, all the diagrams being positive definite. However, this representation introduces other problems, for example it makes the study of the bipolaron at large momentum difficult and inaccurate. In a more general sense, problems appear in all the irreducible channels aside from the one which contains the system ground state (i.e. $K = 0$, singlet). The difficulty is two-fold. First there is the sign problem. Aside from the singlet and $K = 0$ channel where all the terms in Eq. 33 are positive definite, at $K \neq 0$ or/and in the triplet channel the factors $e^{iKx(m)}$ and $g^S(m)$ can take negative values. Second, in the real-space representation we generate all the possible configurations with all the possible symmetries. To project out the lowest energy state of the channel “ γ ” we have to calculate $P_\gamma(\tau)$ up to a time proportional to $1/\Delta_\gamma$, where Δ_γ is the γ channel gap. Therefore we have to simulate larger imaginary times for a channel characterized by a smaller gap. But because all the symmetry channels configurations are generated in the same run, the statistics for the channel γ is proportional to $e^{-(E_\gamma - E_0)\tau}$ (here E_0 is the ground state energy). Thus if the imaginary time is increased, the statistics for channels other than the one which contains the ground state will be exponentially reduced.

Another problem, specific to all ground state projective algorithms, occurs if there are more than one bound state in the same symmetry channel, quasi-degenerate in energy. In this case, at large imaginary time we project out all these states. The results obtained in this case are going to reflect the average of the properties of all the projected states. We encounter this problem at large electron-phonon coupling, where the difference of the s -wave and d -wave bipolaron energies is exponentially small, as the strong coupling theory predicts. However in the intermediate coupling regime we managed to separate these states and we always found a s -wave ground state.

Before we discuss the necessary modifications for adapting our algorithm to other bipolaron models, we mention that, even for the present HH bipolaron, the code can be improved. The momentum K and the spin S are not all the quantum labels which can be used to distinguish between the different symmetry channels. We also have the point group symmetries which break the Hilbert space in different irreducible representations. We have already discussed about s -wave (A_{1g}) and d -wave (B_{1g}) bipolaron states. In principle we can look for all the symmetries given by the representations of the D_{4h} point group. These symmetries can be separated in a similar way to what we did when separating the singlet and the triplet channels. We have to generate diagrams where the time τ is obtained after a translation and a point group operation applied to the time 0. In other words the electronic configurations of the diagrams ends should be connected by a space group operation³³. For every operation there is a certain factor $t^D(m)$ which separates the different representations, and the value of an

observable is calculated analogues to Eq. 33

$$A(K) = \frac{1}{M} \sum_m e^{iKx(m)} g^S(m) t^D(m) a(m) = \frac{\sum_m e^{iKx(m)} g^S(m) t^D(m) w(m) a(m)}{\sum_m w(m)} \quad (45)$$

For example, at $K = 0$, t^D is always 1 for A_{1g} representation. In general t^D should be proportional to the characteristic of the representation. The sign problem can intervene for other representations than A_{1g} . The above approach applied to our present model will improve the accuracy of the results which describe the properties of the s -wave $S1$ bipolaron. However the study of the d -wave symmetry bipolaron will still be difficult and not very accurate, because of the smallness of the binding energy of this state. We believe that no new physics will appear to justify the large coding effort necessary for implementing the above approach. Nevertheless the separation of the different point group representations could be essential for other models which include longer electron-phonon interaction and where strongly bound bipolarons with electrons residing on different sites exist⁹.

The code can be easily modified to include longer range electron-electron and electron-phonon interaction. For an electron-phonon interaction term of the form

$$\sum_{i,j} g_{ij} n_i (b_j^\dagger + b_j) \quad (46)$$

and for an electron-electron interaction of the form

$$\sum_{i,j} V_{ij} n_i n_j \quad (47)$$

there will be no sign problem. The diagrams are similar to the ones shown in Fig. 2 aside from the possibility that now a phonon propagator at site “ j ” can be created or destroyed by an electron at site “ i ”. This process will have a probability equal to $g_{ij} d\tau$. If the two electrons are on sites “ i ” and “ j ” for an interval of time τ a term $e^{-V_{ij}\tau}$ in the diagram weight will correspond.

V. RESULTS

In all the subsequent calculations the phonon energy and the electron hopping term are chosen to be one ($\omega_0 = 1$, $t = 1$). In real materials ω_0 is smaller than t (by almost one order of magnitude), but calculations with such small ω_0 are very time consuming and we find that they do not provide any new qualitative results. Our calculation is done on a 25×25 square lattice with periodic boundary conditions.

A. Phonon Induced Attraction. $U = 0$ Case

With $U = 0$ the effective interaction is always attractive. In Fig. 5 we show the evolution of the system from

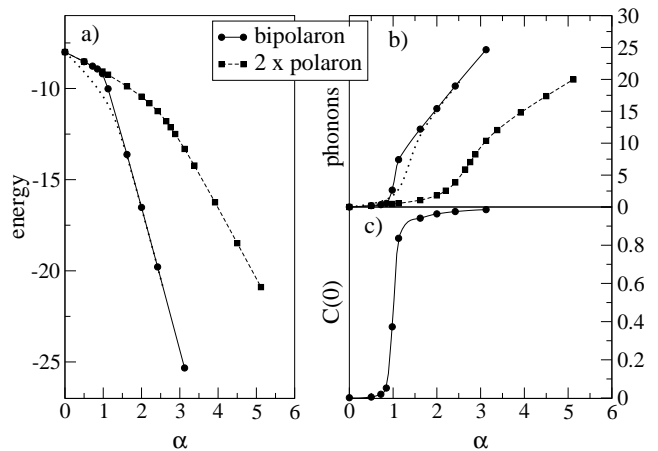


FIG. 5: $U = 0$, $\omega_0 = 1$, $t = 1$. a) The bipolaron energy versus electron-phonon coupling (circles). The dashed line (squares) is $2 \times$ free polaron energy. b) The bipolaron average number of phonons (circles) and $2 \times$ free polaron number of phonons (squares). c) The probability to have the electrons on the same site, $C(0)$, in the bipolaron state. The dotted line in -a (-b) represents the energy (number of phonons) of two free polarons versus the effective coupling, $\alpha_{eff} = 2\alpha$.

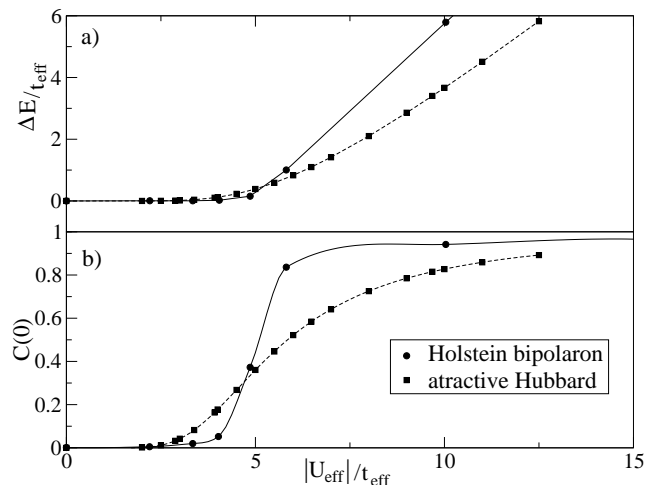


FIG. 6: A comparison between HH bipolaron (solid line) and attractive Hubbard model (dashed line). On the horizontal axis is U_{eff}/t_{eff} , where $U_{eff} = -4\alpha t$ and $t_{eff} = t_{eff}(\alpha)$ is the polaron effective hopping. a) The binding energy in terms of t_{eff} . b) Probability to have two electrons on the same site.

a very weakly bound bipolaron (almost two free polarons) to a strongly bound bipolaron with increasing α . The transition is sharp. It can be seen from Fig. 5-c, where the electrons relative position correlation function $C(r)$ (Eq. 42) is shown at $r = 0$, that in a very short interval around $\alpha_c = 1$ the system ground state changes from almost two free polarons to a state where the electrons are practically on the same site. In comparison to the polaron case, the critical electron-phonon coupling where the transition takes place is approximately two times smaller. This can be understood by noticing that

(see Eq. 10) the deformation energy at a particular site is proportional to the square of the number of electrons on that site. Therefore for the on-site bipolaron the effective α is two times larger than the corresponding polaron one. Thus, the bipolaron energy at a particular coupling α (in the strong coupling regime) is equal to two times the free polaron energy corresponding to a double α . The same is true for the average number of phonons in the bipolaronic cloud (which is also proportional to the square of the number of electrons). This is shown with dotted line in Fig. 5 -a and -b. From the same figures it can also be observed that the bipolaron transition is very sharp compared to the large to small polaron transition³⁴.

In Sec. III we have shown that in the antiadiabatic limit (i.e when $\omega_0 \rightarrow \infty$) the effective attraction induced by phonons becomes instantaneous and as a consequence the HH model is equivalent to a attractive Hubbard model. The attractive Hubbard Hamiltonian was considered as a realistic model to explain the properties of systems like amorphous semiconductors^{25,26,27} or high T_c superconductors⁹ and was under investigation in the past²⁸. However, when the phonon frequency is finite, the interaction becomes retarded and the HH physics will differ from the attractive Hubbard one. Therefore, we think that a comparison of the HH model and the attractive Hubbard model is necessary. Aside from inducing a retarded effective attraction, the other main effect of the electron-phonon interaction is to dress the electrons, increasing their effective mass or equivalently reducing their effective hopping. Consequently, in Fig. 6 we compare the HH Hamiltonian (with $U = 0$) with the corresponding attractive Hubbard model, defined by $U_{eff} = -4\alpha t \equiv -2E_p$ (see Eq. 4 and Eq. 10) and polaron effective hopping $t_{eff} = t_{eff}(\alpha)$. The effective polaron hopping as a function of electron-phonon coupling was calculated numerically with a DQMC code. Increasing U_{eff}/t_{eff} the system evolves in both cases from two free electrons state to a state where the electrons are mainly on the same site ($S0$ bipolaron). At small U_{eff}/t_{eff} , namely when α is smaller than the transition critical α_c , the effective attraction induced by phonons is weaker than the corresponding Hubbard attraction. The transition to the $S0$ bipolaron is very sharp for the HH model, unlike the attractive Hubbard model where it is rather smooth. We found (not shown) that the smaller ω_0 , the sharper the transition is. This is also in agreement with the adiabatic limit calculation ($\omega_0/t \rightarrow 0$) where the transition is of first order¹⁶. Not only is the transition different but also the properties of the bipolaron at large coupling are different in the two cases. The HH $S0$ bipolaron has a large effective mass proportional to t_{eff}^2 , thus with a factor of $e^{4\alpha/\omega_0}$ larger than the free electron mass¹³. On the other hand, the effective mass of the attractive Hubbard bipolaron increases linearly with $|U_{eff}| = 4\alpha t$ in the large U regime, as it can easily be shown analytically.

From both Fig. 5 and Fig. 6 we can conclude that for the HH model there is a very narrow transition region

where the system evolves from two almost free light polarons to a very heavy $S0$ bipolaron. Before the transition, the effect of the electron-phonon interaction is small, especially when the phonon frequency is small. Increasing the phonon frequency results in increasing effective attraction. The physics after the transition is well described by the strong coupling theory. Now the energy and the number of phonons is proportional to α ($E = -8\alpha t$ and $N_{ph} = 8\alpha t/\omega_0$), as it can be seen in Fig. 5-a and -b, and the effective mass is proportional to $e^{4\alpha/\omega_0}$. Unlike the weak coupling regime, here a smaller ω_0 results in a heavier bipolaron state.

B. $S0$ Bipolaron to $S1$ Bipolaron Transition. $U \neq 0$ Case

The weak coupling regime is characterized by the formation of a weakly bound state. The binding energy is extremely small even for $U = 0$, as can be seen from Fig. 5. As discussed in Sec. III A, the bipolaron binding energy decreases rapidly with increasing U , being well below the resolution limit of our algorithm ($10^{-3}t$). Therefore we are not able to determine the critical U where the binding energy reaches zero. However, we do not consider this to be a relevant problem, a bipolaron with such a small binding energy being physically identical with a state of two free polarons.

In the strong coupling regime, as discussed in Sec. III B, with increasing U the system evolves from a strongly bound $S0$ to a weakly bound s -wave $S1$ bipolaron. The $S0$ - $S1$ transition takes place around $U = 2E_p$. At the critical value $U = 4E_p$ the bipolaron state ceased to exist, and the system becomes two polarons moving freely on the lattice. The binding energy of $S0$ bipolaron decreases linearly with U . The $S1$ bipolaron results from the exchange process and its binding energy is proportional to $1/U$ (Eq. 22).

The energy of bipolaron in the intermediate coupling regime is presented in Fig. 7. When $U = 0$ the bipolaron is a $S0$ state. With increasing U the binding energy at first decreases linearly with U and afterwards its behavior changes, decreasing much slower. The bipolaron state disappears well before U reaches $4E_p$. The proportionality to U of the binding energy is a characteristic of the strongly bound $S0$ bipolaron. From Fig. 8 it can be seen that this is correlated with the probability to have the electrons on the same site, $C(0)$ being close to one. At the value of U where the binding energy behavior changes, there is a transition to a weakly bound state (with the binding energy smaller than the one given by the strong coupling theory, Eq. 22) where the probability to have the electrons on neighboring sites is enhanced and where simultaneously $C(0)$ drops to small value. For large couplings, like in Fig. 8-a, this state is a small $S1$ bipolaron, with the electrons residing essentially only on the nearest-neighbor sites. For smaller couplings, as in Fig. 8-d, this state is a "large" $S1$ bipolaron, the wave function being

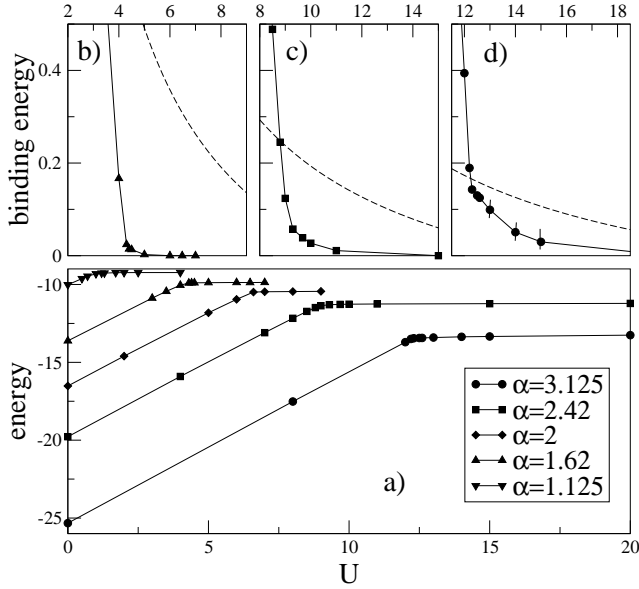


FIG. 7: a) The bipolaron energy versus U for different values of the electron-phonon coupling α . b), c) and d) The binding energy of the bipolaron in the transition region, for $\alpha = 1.62$, $\alpha = 2.42$ and respectively $\alpha = 3.125$, versus U . The dashed line is the $S1$ strong coupling theory predicted binding energy.

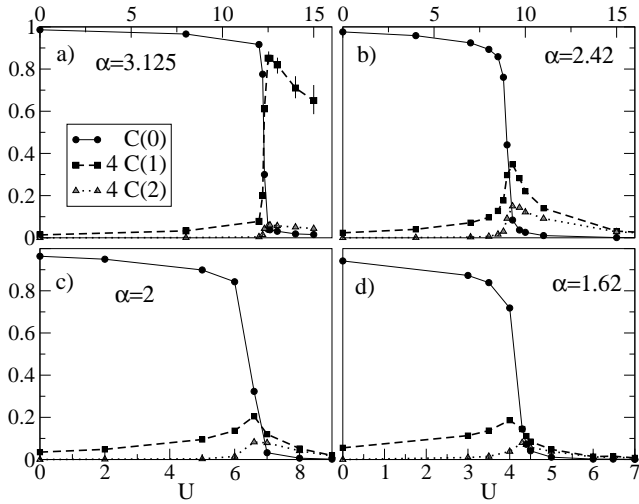


FIG. 8: The electrons position correlation function $C(0)$, $4 \times C(1)$, and $4 \times C(2)$ (see Eq. (42)) versus U for different values of the electron-phonon coupling.

spread over many sites, but still with an enhanced probability that the electrons are nearest-neighbors. This can be seen from Fig. 9, where the correlation function, $C(r)$ (Eq. 42), as a function of the electrons relative distance, r , is shown³⁵.

We know that, in the strong coupling regime for large U , a d -wave $S1$ bipolaron, quasi-degenerate in energy with the s -wave $S1$ ground state exists. When α is large (e.g. $\alpha = 3.125$) our code projects out both $S1$ states at large imaginary time. The results we obtain in this

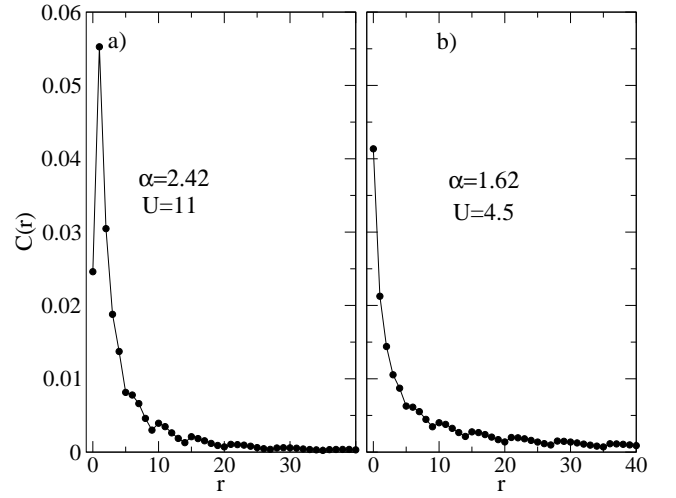


FIG. 9: The correlation function $C(r)$ in the intermediate electron-phonon coupling regime. The relative distance between electrons is given in circular coordinates.

case represent the average of the corresponding two $S1$ bipolarons properties. At smaller couplings the energy difference between the two $S1$ bipolarons is larger and it is easier to project out the ground state and thus to separate the two states. We show this in Fig. 10, where a comparison of the correlation function $C(r)$ measured at two imaginary times, $\tau = 35$ and $\tau = 80$ is made. At time $\tau = 35$ we see a smaller probability for the electrons to stay along the diagonal directions. This is evidence that our measurements capture both the d -wave and the s -wave states. When the measurements are taken at a larger time, the value of the correlation function at sites which correspond to the diagonal directions increases. For the presented case, $C(r)$ does not change sensible if the measurement time is increased above $\tau = 50$, thus we can conclude that the asymptotic regime is reached above this time. The fact that at $\tau = 35$ we see a decrease of $C(5)$, i.e. a decrease of the correlation function at large distance along the diagonal directions, shows that the d -wave bipolaron in the intermediate coupling region is a large state spread over many sites, like the s -wave ground state.

In Fig. 11 we address the $S0$ - $S1$ transition by looking at the number of phonons in the bipolaron cloud and at bipolaron effective mass. Before the $S0$ - $S1$ transition, the number of phonons decreases slowly with U , and it is well approximated by the strong coupling perturbation theory. After the transition the number of phonons is roughly equal to the number of phonons corresponding to two free polarons. The $S0$ - $S1$ transition is sharp, and the bipolaron changes from a very heavy state ($S0$) to a light one ($S1$), as can be seen in Fig. 11-b where the inverse of the bipolaron effective mass is plotted as a function of U . The $S0$ - $S1$ transition is sharp even in the intermediate coupling region. We also have found (not shown) that for smaller ω_0 the transition is sharper. However, we

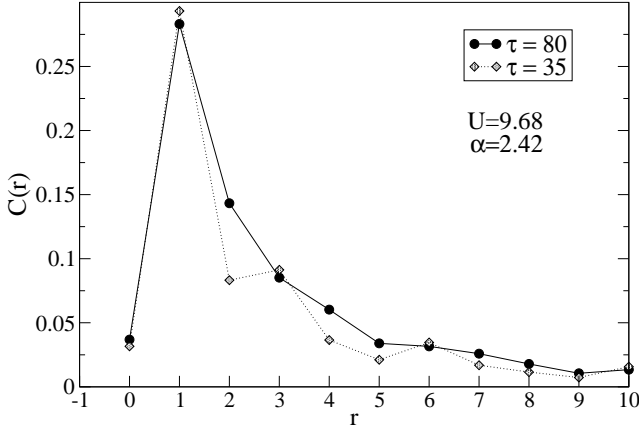


FIG. 10: The correlation function $C(r)$ in the intermediate electron-phonon coupling regime for a value of U which corresponds to a large $S1$ bipolaron. The sites at $r = 2$, $r = 5$ and $r = 9$ are along the diagonal directions. The statistics are collected at two different imaginary times. For the smaller $\tau = 35$ time the results represent the average of the s -wave symmetry ground state and the d -wave symmetry first excited state (notice the small occupation probability of the sites along the diagonal directions). At the larger time, $\tau = 80$, only the s -wave ground state remains.

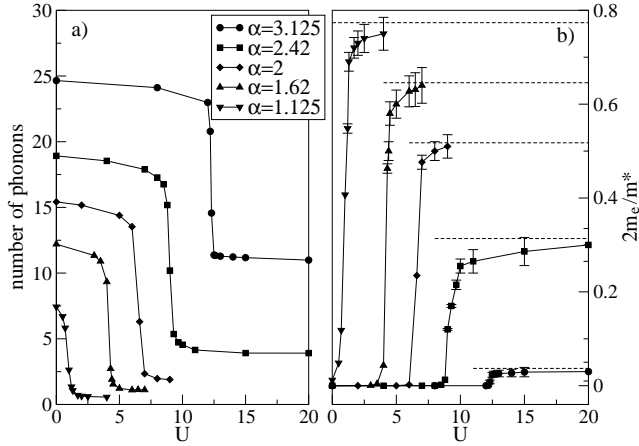


FIG. 11: a) Average number of phonons in the bipolaronic cloud for different values of electron-phonon coupling versus U . b) Inverse of the bipolaron effective mass versus U . m_e is the electron mass. The horizontal lines correspond to the inverse of *two free polarons* effective mass.

want to specify that when we talk about transition we mean a continuous change of system properties and not a non-analytical jump.

To conclude, in the intermediate coupling regime, with increasing U , the system evolves continuously from a heavy, strongly bound $S0$ bipolaron to a light, weakly bound state spread over many sites. This state, which we call large $S1$ bipolaron, has s -wave symmetry and an enhanced probability that the electrons occupy nearest-neighbor sites. In the same region of parameters another stable state with d -wave symmetry exists, with a

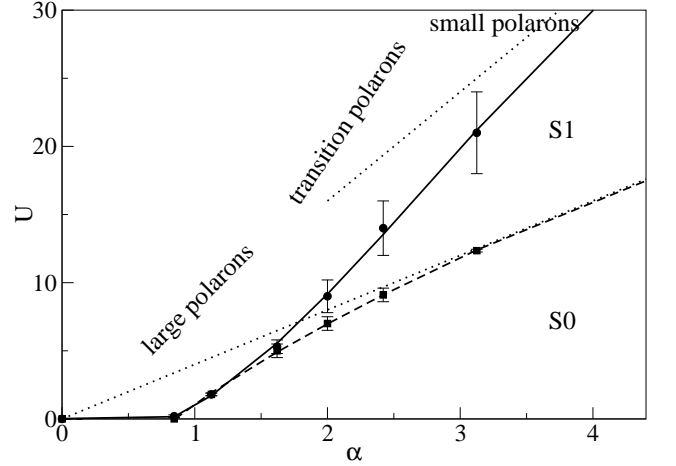


FIG. 12: Phase diagram. The solid line is the *bipolaron -two free polarons* boundary. The dashed line separates the $S0$ and $S1$ bipolarons. The dotted lines are the strong coupling theory results.

smaller binding energy. The spatial extent of this state is also large. When α is increased both s -wave $S1$ and d -wave $S1$ bipolaron wave functions become more localized evolving to the states predicted by the perturbation theory. The energy difference between the s -wave and the d -wave states becomes exponentially small at large electron-phonon coupling.

The results presented up to here are calculated for $K = 0$ and in the singlet channel. For the strongly bound $S0$ bipolaron, in agreement with the exponentially small effective hopping predicted by the perturbation theory, we found a flat dispersion resulting in a narrow band, of the order of the calculation error bars. We are not able to compute the momentum dependent properties of the weakly bound bipolarons for reasons described in Sec. IV C. In the triplet channel we found no bound states for any value of the parameters.

C. Phase Diagram

The phase diagram is shown in Fig. 12. We want to remind the reader that with our technique, the calculation becomes difficult when the binding energy is small. The smaller is the binding energy, the larger time computations are needed. The most difficult computations are at both large electron-phonon coupling and large U . The large imaginary time simulations are difficult because the number of phonons and the effective mass is always large in this case (the ground state consists of two weakly interacting small polarons, and a small polaron has itself an exponentially large mass and contains a large number of phonons). Therefore the largest errors we get are in the determination of the *bipolaron -two free polarons* boundary at large values of α . In the strong coupling theory this boundary is determined by the critical value

$U = 8\alpha t \equiv 4E_p$. In the intermediate coupling regime we find that the bipolaron state disappears much before that value. The value $U = 8\alpha t \equiv 4E_p$ should be taken as an upper limit for the existence of the bipolaron state, reached asymptotically when α is increased.

The $S1$ region contains a weakly bound state where the probability to have the electrons on nearest-neighbor sites is larger than of having them on the same site. Depending on the value of electron-phonon coupling the $S1$ bipolaron can be a large state with the wave function spread over many sites, or a small state where the electrons are residing on nearest-neighbor sites. The large $S1$ bipolaron breaks into two large or intermediate (transition) polarons and the small $S1$ bipolaron evolves into two small polarons with increasing the Coulomb repulsion U . The $S1$ bipolaron is a state which forms only at intermediate and large electron-phonon coupling, thus only where the polaron kinetic energy is strongly reduced. In this region, the exchange attraction which is weakly renormalized by the phonons, can overcome the effective kinetic energy resulting in the formation of the $S1$ bound state.

At small α , the binding energy is extremely small, well beyond the resolution limit of our algorithm, and decreases rapidly with increasing U . The maximum critical U where the bipolaron breaks can be theoretically as large as $U = 4\alpha t \equiv 2E_p$, but for U larger than the boundary shown in Fig. 12 the binding energy is so small that can be safely approximated by zero.

VI. CONCLUSIONS

In this paper we studied the two-dimensional HH bipolaron using a Diagrammatic Quantum Monte Carlo algorithm which computes the zero temperature Matsubara Green's functions. The bipolaron properties are extracted from the Green's functions behavior at large imaginary time where the ground state is projected out. Unlike the other DQMC simulations used for studying different polaron and exciton models, in order to avoid the sign problem, our algorithm produces and sums real space (Wannier orbitals basis) diagrams. The code can be relative easily modified for other bipolaron models with longer range electron-phonon and/or electron-electron interaction. The dimensionality and the lattice symmetry can also be modified.

We calculated the phase diagram in the parameter space defined by U and α . Depending on the parameters value, different kinds of bound states are formed. We studied both their properties and the transition from one bipolaron type to another.

At small electron-phonon coupling two electrons form an extremely weakly bound state when $U = 0$. In this regime the binding energy decreases fast with increasing the Coulomb repulsion and increases with increasing phonon frequency.

For larger couplings, depending on the value of U , the phonon-induced attraction may result in the formation of a strongly bound $S0$ bipolaron or of a weakly bound $S1$ bipolaron. The $S0$ bipolaron forms at small values of U , for couplings larger than $\alpha_c \approx 1$. It is an on-site state and its properties are well described by the strong coupling perturbation theory. With increasing U , around the value given by the strong coupling perturbation theory ($U = 2E_p$), the $S0$ bipolaron transforms sharply (but continuously) into a weakly bound state with an enhanced probability to have the electrons on nearest-neighbor sites, called $S1$ bipolaron. The $S1$ bipolaron is a large state spread over many lattice sites for α in the intermediate regime (which corresponds to polaron transition region), and becomes nearest-neighbor localized at large α . The unrenormalized exchange energy which wins over the reduced polaron effective hopping is responsible for binding the $S1$ bipolaron. The binding energy of the $S1$ bipolaron and the critical Coulomb repulsion U where the bipolaron state disappears are smaller than the values obtained in the strong coupling perturbation theory ($U = 4E_p$).

We found that the ground state always has s -wave symmetry. In the intermediate and strong electron-phonon coupling regime, for values of U which correspond to the $S1$ ground state, an excited d -wave stable state also exists. This state is spatially large for intermediate α and nearest-neighbor localized for large α , similar to the corresponding s -wave ground state. The excitation energy (difference between the d -wave and s -wave $S1$ states) is larger at intermediate coupling and goes exponentially to zero when α is increased.

ACKNOWLEDGMENT

We want to thank N. Prokof'ev, A.S. Mishchenko, M. Mostovoi, D. Khomskii and S. A. Trugman for useful discussions related to bipolarons and polarons. We are particularly grateful the first two of them for their help in developing the DQMC code. The work was supported by the Netherlands Foundation for Fundamental Research on Matter (FOM) with financial support from the Netherlands Organization for Scientific Research (NWO) and the Spinoza Prize Program of NWO and by NSF grants DMR-0073308 and DMR-0113574.

¹ C. Schlenker, *Physics of Disordered Materials*, edited by D. Adler, H. Fritzsche and S. Ovshinski (Plenum, New York,

1985)

² S.Tajima, *et al.*, Phys.Rev.B **35**, 696 (1987)

- ³ J. Scott, J.L. Bredas, J.H. Kaufman, P. Pfluger, S.B. Street and K. Yakhusli, *Mol. Cryst. Liq. Cryst.* **118**, 163 (1983)
- ⁴ A. Lanzara, *et al.*, *Phys.Rev.Lett.* **81**, 878 (1998); Guo-Meng-Zhao, *et al.*, *Nature* **381**, 676 (1996); K.H. Kim, *et al.*, *Phys.Rev.Lett.* **77**, 1877 (1996); A.J. Millis, P.B. Littlewood and B.I. Shraiman, *Phys.Rev.Lett.* **74**, 5144 (1995); A.J. Millis, *Nature (London)* **392**, 147 (1998)
- ⁵ S. Lupi, *et al.*, *Phys.Rev.Lett.* **83**, 4852 (1999); E.S. Bozin, *et al.*, *Phys.Rev.Lett.* **84**, 5856 (2000); A. Bianconi, *et al.*, *Phys.Rev.Lett.* **76**, 3412 (1996)
- ⁶ L.D. Landau, *Z.Phys.* **3**, 664 (1933)
- ⁷ J. Bardeen, L.N. Cooper and J.R. Schrieffer, *Phys.Rev.* **108**, 1175 (1957)
- ⁸ A. B. Migdal, *Sov. Phys. JETP* **7**, 996 (1958), G. M. Eliashberg, *Sov. Phys. JETP* **11**, 696 (1960), G. M. Eliashberg, *Sov. Phys. JETP* **12**, 1000 (1960)
- ⁹ A. S. Alexandrov and N. F. Mott, *Rep. Prog. Phys.* **57**, 1197 (1994)
- ¹⁰ A.S. Alexandrov, V. V. Kabanov and D. K. Ray, *Phys.Rev.B* **49**, 9915 (1994)
- ¹¹ A.S. Alexandrov, *Phys.Rev.B* **53**, 2863 (1995); A.S. Alexandrov and P.P. Edwards, *Physica C* **331**, 97 (2000)
- ¹² B. K. Chakraverty, J. Ranninger and D. Feinberg, *Phys. Rev. Lett.* **81**, 433 (1998).
- ¹³ J. Bonča, T. Katrašnik and S.A. Trugman, *Phys.Rev.Lett.* **84**, 3153 (2000)
- ¹⁴ A. La Magna and R. Pucci, *Phys.Rev.B* **55**, 14886 (1997)
- ¹⁵ G. Wellein, H. Roder and H. Fehske, *Phys.Rev.B* **53**, 9666 (1996); A. Weisse, H. Fehske, G. Wellein and A.R. Bishop, *Phys.Rev.B* **62**, 747 (2000)
- ¹⁶ L. Proville and S. Aubry, *Physica D* **133**, 307 (1998), *Eur.Phys.J B* **11**, 41 (1999)
- ¹⁷ G.De Filippis, V. Cataudella, G. Iadonisi, V.M. Ramaglia, C.A. Perroni and F. Ventriglia, *cond-mat/0106586*
- ¹⁸ N. Prokof'ev, B. Svistunov, and I. Tupitsyn, *JETP* **87**, 310 (1998).
- ¹⁹ N.V. Prokof'ev and B.V. Svistunov, *Phys.Rev.Lett.* **81**, 2514 (1998); A.S. Mishchenko, N.V. Prokof'ev, A.Sakamoto and B.V. Svistunov, *Phys.Rev.B* **62**, 6317 (2000)
- ²⁰ A.S. Mishchenko, N.V. Prokof'ev and B.V. Svistunov, *Phys.Rev.B* **64**, 033101 (2001)
- ²¹ E.A. Burovski, A.S. Mishchenko, N.V. Prokof'ev and B.V. Svistunov, *Phys.Rev.Lett.* **87**, 186402 (2001)
- ²² J. Bonča and S.A. Trugman, *Phys.Rev.B* **64**, 094507 (2001)
- ²³ I. G. Lang and Yu. A. Firsov, *Sov. Phys. JETP* **16**, 1301 (1963)
- ²⁴ N. Metropolis, A.W. Rosenbluth, M.N. Rosenbluth, A.M. Teller and E. Teller, *J. Chem. Phys.* **21**, 1087 (1953)
- ²⁵ P.W. Anderson, *Phys.Rev.Lett.* **34**, 953 (1975)
- ²⁶ R.A. Street and N. F. Mott, *Phys.Rev.Lett.* **35**, 1293 (1975)
- ²⁷ D. Alder and E. J. Yoffa, *Phys.Rev.Lett.* **36**, 1197 (1976)
- ²⁸ S. Robaszkiewicz, R. Micnas and K.A. Chao, *Phys.Rev.B* **23**, 1447 (1981); *Phys.Rev.B* **24**, 1579 (1981)
- ²⁹ C. Kittel, *Introduction to solid state physics* (New-York, 1996)
- ³⁰ However the reader should be aware that HH model is presumably not the best candidate to address the physics of cuprate superconductors, at intermediate and large electron-phonon coupling producing bipolarons with extremely large effective mass¹². Models with longer range electron-phonon interaction²² are believed to be more realistic for describing cuprates.
- ³¹ Migdal's theorem shows that the vertex corrections are of order ω_0/ε_F due to Pauli exclusion principle which blocks the electron-phonon scattering inside the Fermi sea.
- ³² Other authors define the dimensionless coupling constant as the ratio between the deformation energy and the phonon frequency²⁹, which will be a measure of the number of phonons in the polaron cloud. If in BCS theory of superconductivity the approximation $N(0) \approx 1/2W$ is made, where $N(0)$ is the density of states at the Fermi level and W is the electron bandwidth, the relation of our α to the BCS electron-phonon coupling, $\lambda = 2g^2/\omega_0N(0)$, will be $\alpha = 2\lambda$.
- ³³ In fact the separation of singlet and triplet obeys the same idea, the permutation group operations being used.
- ³⁴ The Holstein polaron properties were calculated with a DQMC code similar to the one presented in¹⁹ and used for the Fröhlich polaron study.
- ³⁵ Notice that the total probability to have the electrons at the distance r from each other is $C(r)$ times the number of sites situated at the relative distance r . Therefore, in Fig. 8, we plotted $4 \times C(1)$ and $4 \times C(2)$ which represent the probability to have the electrons on nearest and respectively next-nearest neighbor sites.